PLANT SCIENCE TODAY
Vol 13(1): 1-17
https://doi.org/10.14719/pst.10194

eISSN 2348-1900

RESEARCH ARTICLE

Plant-derived coagulants as sustainable alternative for aquaculture wastewater cleanup

Chandana Chintu[1], Harshitha Marla[1], Saritha Vara[2] & Patnala Kiranmayi[1*]

[1]Department of Life Sciences, Biotechnology Division, Gandhi Institute of Technology and Management (Deemed to be University),Visakhapatnam 530 045, Andhra Pradesh, India
[2]Department of Life Sciences, Environmental Science Division, Gandhi Institute of Technology and Management (Deemed to be University), Visakhapatnam 530 045, Andhra Pradesh, India

*Correspondence email - kpatnala@gitam.edu

Received: 23 June 2025; Accepted: 04 September 2025; Available online: Version 1.0: 02 January 2026; Version 2.0: 19 January 2026

Cite this article: Chandana C, Harshitha M, Saritha V, Patnala K. Plant-derived coagulants as sustainable alternative for aquaculture wastewater cleanup. Plant Science Today. 2026; 13(1): 1-17. https://doi.org/10.14719/pst.10194

Abstract

The rapid increase in population and the ongoing depletion of freshwater resources have raised global concerns about water scarcity. In response to this critical issue, there is an urgent need to reuse wastewater by removing contaminants. Chemical coagulants have been excessively used due to their high efficiency, but they come with disadvantages. In this study, a novel approach was explored by utilizing the whole plant (leaves, stem and roots) of two underexplored medicinal plants, *Catharanthus roseus* and *Ocimum tenuiflorum,* to evaluate their efficiency in treating aquaculture wastewater. Coagulation experiments were conducted using jar test apparatus. Adsorption of the pollutants on the coagulants through sweep flocculation, pore entrapment and charge neutralization mechanisms were observed through Scanning Electron Microscope (SEM) studies. Attenuated Total Reflectance - Fourier Transform Infrared (ATR-FTIR) analysis revealed the key functional groups -OH, C=C and C=N on the coagulants that contributed to flocculation of pollutants. The overall experimental study revealed that all coagulant types were efficient in treating aquaculture wastewater at an optimal dose range of 0.3-0.4 g/L. *Catharanthus roseus* roots were better at removing turbidity (99 %) followed by total suspended solids (98.3 %) and total dissolved solids (96.3 %). Chlorides, sulphates, phosphates and nitrates were efficiently removed with a blend of *C. roseus* and *O. tenuiflorum.* Electrical conductivity was reduced effectively by up to 99 % with *O. tenuiflorum* seeds. These overall findings indicate an eco-friendly, sustainable solution for aquaculture wastewater treatment.

Keywords: ATR-FTIR; *C. roseus*; coagulation/flocculation; FE-SEM; *O. tenuiflorum*; plant-based coagulants

Introduction

Aquaculture has emerged as one of the fastest-growing sectors in the global food production industry, contributing significantly to rural livelihoods and global food security (1). However, the rapid expansion of this industry has led to environmental issues, notably the release of untreated or improperly managed wastewater (2). Wastewater generation in aquaculture is a result of the operation of hatcheries and farming systems (3). Aquaculture effluents are abundant with organic matter, uneaten feed, fecal waste, nitrogen, phosphorus, occasional antibiotics and detrimental microbes (4). Nitrate and phosphate pollution in wastewater occurs due to agricultural run-off, sewage, atmospheric deposition, urban run-off, industrial wastewater and aquaculture effluents (5). If these contaminants are discharged into natural water bodies, they can cause eutrophication, depletion of the oxygen level and biodegradation of soil and aquatic ecosystems (6). In order to support a sustainable sector and a circular economy, aquaculture contaminants should be properly processed for reuse in different applications or safely released into the environment (7). Regular traditional methods like chemical coagulation, sedimentation and advanced filtration depend on synthetic materials like alum and ferric chloride, which are expensive, non-biodegradable and dangerous to the environment (8).

In recent years, to mitigate this toxicity caused by synthetic coagulants, researchers and environmentalists have focused on cost-effective and eco-friendly sources for treating aquaculture wastewater (9). Plant-based natural coagulants, particularly those derived from medicinal and indigenous plants, are promising alternatives because of their eco-friendliness, biodegradability, local availability and cost-effectiveness (10). Many of the plants contain bioactive compounds such as tannins, alkaloids, saponins and flavonoids, which can help in coagulation and the removal of impurities from the wastewater (11). *Catharanthus roseus* (commonly known as Madagascar periwinkle) and *Ocimum tenuiflorum* (commonly known as Tulasi - holy basil) are two medicinal plants that are available locally and are a rich source of bioactive compounds (12, 13). Both plants are known for their anti-microbial, antioxidant, anti-inflammatory and phytochemical properties (14, 15). In previous studies, it has been shown that these plant extracts can be used to remove the organic waste and pathogenic microorganisms that are present in the water (16). But there is limited research on

using these specific plant natural coagulants for treating aquaculture wastewater, which is unique when compared with industrial wastewater treatment (17).

This work aims to investigate the effectiveness of using *C. roseus* (CR) and *O. tenuiflorum* (OT) plants as natural coagulants in treating the aquaculture wastewater collected from the Visakhapatnam north coastal hatcheries. The treatment performance is evaluated by measuring water quality parameters such as pH, electrical conductivity, turbidity, total solids, total dissolved solids, hardness, chlorides, sulphates, phosphates and nitrates before and after treatment with different concentrations of these plant-based natural coagulants. Jar test experiments were conducted and the natural coagulants were dried and analyzed using field emission scanning electron Microscope (FE-SEM) and attenuated total reflectance - Fourier transform infrared (ATR-FTIR) analysis to study surface changes and chemical composition.

Materials and Methods

Aquaculture wastewater sample collection

Aquaculture wastewater samples were obtained from Rajkamal shrimp hatcheries, located approximately 3.5 km from GITAM (Deemed to be University), Visakhapatnam. Samples were collected in four pre-cleaned jerry cans each filled to the brim to prevent air entrapment and minimize oxidative changes during transport. The cans were securely sealed, appropriately labelled, safely transported to the laboratory and stored at 4 °C under refrigeration for further analysis.

Bio-coagulant preparation

Catharanthus roseus and *O. tenuiflorum* plants were carefully uprooted from sites near aquaculture farms. The collected plants were thoroughly washed under running tap water, followed by rinsing with deionized water to remove adhering soil particles and other surface impurities. The plant materials were segregated into stems, leaves and roots and dried in a hot-air oven at 60 °C for 72 hr to ensure complete elimination of moisture. Once dried, each plant part was ground into a fine powder and sieved using a 0.50 mm sieve to obtain a consistent size to use as a bio-coagulant.

Coagulation studies

Coagulation experiments were conducted using a conventional Jar test apparatus under controlled laboratory conditions at 27 ° C. Each experimental run utilized 1 L of untreated aquaculture wastewater and the performance of each bio-coagulant was evaluated independently. To determine the optimal dosage for maximum removal efficiency, a range of coagulant concentrations (0.2, 0.4, 0.6, 0.8 and 1.0 g/L) was systematically tested in triplicates for *C. roseus*, *O. tenuiflorum* and a 1:1 mix of *C. roseus* and *O. tenuiflorum*. The Jar test process involved three sequential stages (i) flash mixing at 80 rpm for 2 min to ensure uniform dispersion of the coagulant, (ii) slow mixing (flocculation) at 30 rpm for 30 min to promote floc formation and (iii) settling period of 30 min to allow flocs sedimentation. Following settling, the clarified supernatant was carefully decanted, filtered and analyzed to assess the effect of coagulant dose on the pollutant removal efficiency of aquaculture wastewater, using the formula (Eqn. 1):

$$RE\ (\%) = \frac{ci - cf}{ci} \times 100 \qquad \text{(Eqn. 1)}$$

Where, RE % = removal efficiency percentage, Ci = initial concentration before coagulation, Cf = final concentration after coagulation.

Analytical parameters

The key water quality parameters, including pH, electrical conductivity (EC), turbidity (TU), total suspended solids (TSS), total dissolved solids (TDS), total hardness (TH), chlorides, nitrates, phosphates and sulphates were analyzed as per the American Public Health Association (APHA) 2016 standard methods (18).

pH

pH of the collected wastewater samples was measured using a digital pH meter. Prior to the start of the experiment, the electrodes were calibrated with standard buffer solutions of pH 4.6 and 9.3 to ensure accurate results. After calibration, the electrodes were thoroughly rinsed with distilled water for the removal of any residual buffer, gently dried with tissue paper and immersed in the water samples to record the stabilized pH values (19).

Electrical conductivity (EC)

Electrical conductivity (EC) of the samples was measured using a digital conductivity meter, calibrated with 0.1 N potassium chloride (KCl) solution having a conductivity of 14.12 mmho/cm. The electrodes were rinsed with deionized water, dried and then immersed in the water sample to record the stabilized readings (19).

Turbidity

The nephelometric turbidimeter is used to check the turbidity of the water samples, with results expressed in NTU (nephelometric turbidity units). The instrument was initially calibrated using a standard suspension of 40 NTU and the scale was adjusted to 100 as a reference. Water samples were thoroughly mixed and filled into clean cuvettes, after which stabilized turbidity values were recorded (19).

Total suspended solids (TSS)

Total suspended solids were determined using a gravimetric method. Clean, dry Petri dishes were preheated in a hot-air oven, allowed to cool to room temperature and their initial weights (Wi) were recorded. Subsequently, 10 mL of the sample was added to each plate and evaporated in a hot air oven at 100 °C for 1 hr. After evaporation, the Petri plates were cooled and reweighed to obtain the final weight (Wf). The concentration of TSS was calculated using the formula (Eqn. 2) (19):

$$TSS = \frac{(Wf) - (Wi)}{V} \times 1000 \qquad \text{(Eqn. 2)}$$

Where, Wi = initial weight of Petri plate (mg), Wf = final weight of Petri plate (mg), V = volume of the sample (mL).

Total dissolved solids (TDS)

Total dissolved solids were assessed using a gravimetric method. Clean, dry Petri dishes were preheated in a hot-air oven, cooled to room temperature and their initial weights (Wi) were recorded. A 10 mL of the water sample was filtered using Whatman filter paper and the filtrate was transferred to the pre-weighed dishes. The

samples were then evaporated at 100 °C for 1 hr in a hot-air oven. Following evaporation, the Petri plates were cooled and reweighed to determine the final weight (Wf). The concentration of TDS was calculated using the formula (Eqn. 3) (19):

$$TDS = \frac{(Wf) - (Wi)}{V} \times 1000 \qquad \text{(Eqn. 3)}$$

Where, Wi = initial weight of Petri plate (mg), Wf = final weight of Petri plate (mg), V = volume of the sample (mL).

Total hardness (TH)

Total hardness was determined by titration using ethylenediaminetetraacetic acid (EDTA). A 100 mL aliquot of the sample was transferred to a conical flask, followed by the addition of 2 mL buffer solution and 2 drops of Eriochrome black T indicator, which instantly turned the solution to a wine-red color. The sample was then titrated with 0.01 M EDTA until the color changed from wine-red to blue, indicating the endpoint. A blank titration was performed under similar conditions. The volumes of EDTA used for sample (A) and blank (B) were recorded and the total hardness was calculated using the formula (Eqn. 4) (19):

$$TH = \frac{A - B}{V} \times 1000 \qquad \text{(Eqn. 4)}$$

Where, A = volume of EDTA used for the sample (mL), B = volume of EDTA used for the blank (mL), V = volume of the sample (mL).

Calcium hardness (CH)

Calcium hardness was measured by taking a 100 mL aliquot of the sample in a conical flask with 1 mL NaOH (sodium hydroxide) and a pinch of murexide indicator, which caused the solution to change to pink immediately. Later, the sample was titrated with 0.01 M EDTA until the color shifted from pink to blue, followed by the titration of the blank. The volumes of EDTA utilized for sample (A) and blank (B) were noted and calcium hardness was calculated using the formula (Eqn. 5) (19):

$$CH = \frac{A1 \times 1000}{V} \qquad \text{(Eqn. 5)}$$

Where, A1 = volume of EDTA used for the sample (mL), V = volume of the sample (mL).

Chlorides

For chloride estimation, 10 mL of the water sample was taken into a conical flask, followed by the addition of 2 drops of potassium chromate indicator, which imparted a pale-yellow color. The sample was then titrated with standard silver nitrate ($AgNO_3$) until a brick-red endpoint was reached. A blank was also titrated under identical conditions. The volume of $AgNO_3$ consumed for both sample (A) and blank (B) was recorded and the chloride concentration was calculated with the formula (Eqn. 6) (19):

$$Chlorides = \frac{(A - B) \times N \times 35.46}{V} X\ 100 \qquad \text{(Eqn. 6)}$$

Where, A = volume of $AgNO_3$ used for the sample (mL), B = volume of $AgNO_3$ used for the blank (mL), N = normality of silver nitrate, V = volume of the sample (mL).

Sulphates

Total sulphate concentration was estimated by mixing 5 mL of the water sample with 5 mL conditioning reagent, followed by dilution with 90 mL distilled water. Subsequently, 1 g of barium chloride ($BaCl_2$) was added and stirred thoroughly for uniform dispersion. Later, the absorbance of the resulting solution was measured at 420 nm using a UV-visible spectrophotometer and the values are recorded (19).

Phosphates

For phosphate estimation, 5 mL of the water sample was taken and a drop of phenolphthalein indicator was added. Sulfuric acid was added dropwise until the pink color disappeared. The sample was then boiled for approximately 1.5 hr, cooled and neutralized with NaOH until a faint pink color reappeared. The solution was filtered and 50 mL of the filtrate was transferred to a volumetric flask. To this, 2 mL of ammonium molybdate and 0.5 mL of stannous chloride were added and the volume was made up to 100 mL with distilled water. The intensity of the developed color was measured at 690 nm using a UV-visible spectrophotometer (19).

Nitrates

For nitrate estimation, 10 mL of the filtered water sample was transferred to a clean Petri dish and evaporated to dryness in a hot air oven at 120 °C for 2 hr. After cooling, the residue was collected in a beaker and dissolved in 2 mL of phenol disulphonic acid (PDA) and the final volume was made up to 50 mL with distilled water. Subsequently, 10 mL of concentrated liquid ammonia was added to develop a yellow coloration. The absorbance of the resulting solution was measured at 410 nm using a UV-visible spectrophotometer to determine nitrate concentration (19).

Results and Discussion

Physicochemical parameters

The initial freshwater that is taken for cultivating shrimp and the final wastewater generated after cultivation was tested to study their differences in physicochemical properties. Results are shown in Table 1, where changes can be observed in all the key water parameters of pH, turbidity, EC, TSS, TDS, TH, CH, chlorides, sulphates, phosphates and nitrates. Slight changes in pH and turbidity between freshwater and wastewater can be observed, with pH rising from 7.4 to 8.36, turbidity from 4.4 to 4.8 and phosphate levels increasing to 10.35 from 7.35 mg/L. A moderate increase in EC, TH, sulphates and nitrates is visible, with significant differences in levels of TSS, TDS, CH and chlorides. Various factors, such as metabolic activity, nitrification, shrimp feed, dissolved oxygen, uneaten food, feces and accumulation of organic waste, often result in the complete shift of water parameters to a higher value (4).

Bio-coagulant pollutant removal efficiency study

Firstly, in order to simplify and avoid confusion regarding the samples, they are designated with the following short forms: CRL - *C. roseus* leaf, CRS - *C. roseus* stem, CRR - *C. roseus* root , OTL - *O. tenuiflorum* leaf, OTS - *O. tenuiflorum* stem, OTR - *O. tenuiflorum* root, COL - blend of *C. roseus* and *O. tenuiflorum* leaves, COS - blend of *C. roseus* and *O. tenuiflorum* stems, COR - blend of *C. roseus* and *O. tenuiflorum* roots.

The overall experimental findings demonstrated the

Table 1. Physicochemical parameters of fresh water and raw aquaculture wastewater

Physicochemical parameters	Fresh water sample	Wastewater sample	Analysis method
pH	7.43 ± 0.3	8.36 ± 0.1	pH meter
EC (mmho/cm)	3.5 ± 0.2	15.6 ± 0.1	2520-B
Turbidity (NTU)	4.4 ± 0.3	4.8 ± 0.1	Turbidimeter
TSS (mg/L)	45,800 ± 1.2	2,42,600 ± 2.8	2540-D
TDS (mg/L)	39,200 ± 0.7	75,700 ± 1.1	2540-C
TH (mg/L)	5,000 ± 0.3	5,900 ± 0.3	2340-C
CH (mg/L)	100 ± 0.1	1,500 ± 0.1	2340-C
Chlorides (mg/L)	3,377 ± 0.7	11,819 ± 0.9	4500-Cl^- B
Sulphates (mg/L)	20.32 ± 0.2	33.90 ± 0.1	4500 SO_4^{2-} E
Phosphate (mg/L)	7.39 ± 0.1	10.35 ± 0.1	4500-P D
Nitrates (mg/L)	0.098 ± 0.01	0.311 ± 0.01	4500 NO_3^- B

potential of all the tested coagulants to effectively adsorb and remove contaminants from aquaculture wastewater. Analysis of the results revealed that the adsorption efficiency varied among different coagulants, with each revealing optimal performance at different dosages. The pollutant removal efficiency (%) of all the coagulants across varying concentrations from 0.1 to 0.5 g/L for each assessed water quality parameter were represented in Fig. 1-11.

The variations in pH after treating raw aquaculture wastewater are presented in Fig. 1. The pH significantly decreased from 8.3 to 4.6, 5.4 and 4.3 with COL, COS and COR, respectively. However, CRL led to an increase in pH, raising its value from 8.3 to 9.0 at a dosage of 5 g/L. In the majority of coagulants, an increase in dosage led to a decrease in pH or a very slight change in its value.

Fig. 2 shows the reduction in electrical conductivity with the highest removal of 99.3 % observed with CRS at a dosage of 0.4 g/L, followed by CRL and CRR with 99.1 % and 96 % at a dosage of 0.3 g/L. *Moringa oleifera* seeds and cactus (*Opuntia*) caused a lesser increase in conductivity of about 38 % and 36 %, respectively (20). Blended coagulants like alum and chitin showed the highest EC removal up to 58.85 %, while a combination of alum, chitin and sago was most stable, achieving 48.85 % (21). Another study on *M. oleifera* and chitin exhibited a reduction of 66.49 % in EC (9).

Turbidity, TSS and TDS removal

Turbidity of aquaculture wastewater is associated with an increase in suspended solids. In our study all the tested coagulants were able to efficiently reduce turbidity (Fig. 3). *Catharanthus roseus* stem (CRS) was able to remove turbidity from wastewater by 99 % with a dose of 0.3 g/L. An experiment performed using *M. oleifera* seeds showed maximum turbidity reduction at an optimal dosage of 20 mg/L for 5 NTU turbidity and 230 mg/L for 300 NTU turbidity (22). Other experiments conducted on sorghum coagulant revealed 87.73 % removal, while sugarcane bagasse exhibited 95.9 % removal (23, 24). Apart from natural coagulants, chemical coagulants such as alum achieved 99.08 % turbidity removal, while alum in conjugation with *Carica papaya* seeds achieved 100 % turbidity removal (25, 26).

Fig. 4 displays the removal efficiency of the TSS. *Catharanthus roseus* root (CRR) and CRL exhibited the highest removal efficiency with 99 % at 0.4 g/L and 0.3 g/L, respectively. Almost all the coagulants were able to remove total suspended solids with greater than 90 % efficiency in varying dosages of 0.3 g/L to 0.5 g/L. Alum, a common chemical coagulant, displayed a removal efficiency of 98.71 %, which was close to our findings of 99 % reduction. Similarly, *M. oleifera* seeds powder along with neem, cassava and wild betel leaves showed 80.28 % removal (27). Chitosan, a bio-coagulant, exhibited the highest removal capacity of 88.84 % at a dose of 0.4 g/ L (28).

Higher TDS removal efficiency was achieved by CRR at a dosage of 0.5 g/L (Fig. 5). CRL, OTL and COR were also able to clear the dissolved solids with an efficiency greater than 90 % at dose ranges of 0.3-0.4 g/L. *Moringa oleifera* seed powder has succeeded in treating municipal sewage water by reducing TDS up to 76 % but failed to treat TDS in aquaculture wastewater (9). However, *M. oleifera,* when blended with other coagulants such as *Aloe vera*, exhibited TDS removal of 74 % with a dose of 0.1 g/L and 92.1 % (9, 29).

Total hardness and calcium hardness removal

Fig. 6 represents the total hardness removal percentages of all the coagulants studied. Total hardness (TH) was efficiently removed up to 92 % and 94 % by OTR and COL at a dosage of 0.5 g/L. The maximum calcium hardness removed was 89 % with COL at a dosage of 0.5 g/L (Fig. 7). Total hardness and calcium hardness removal were better achieved with a blend of *Catharanthus* and *Ocimum* leaves at a dosage of 0.5 g/L,

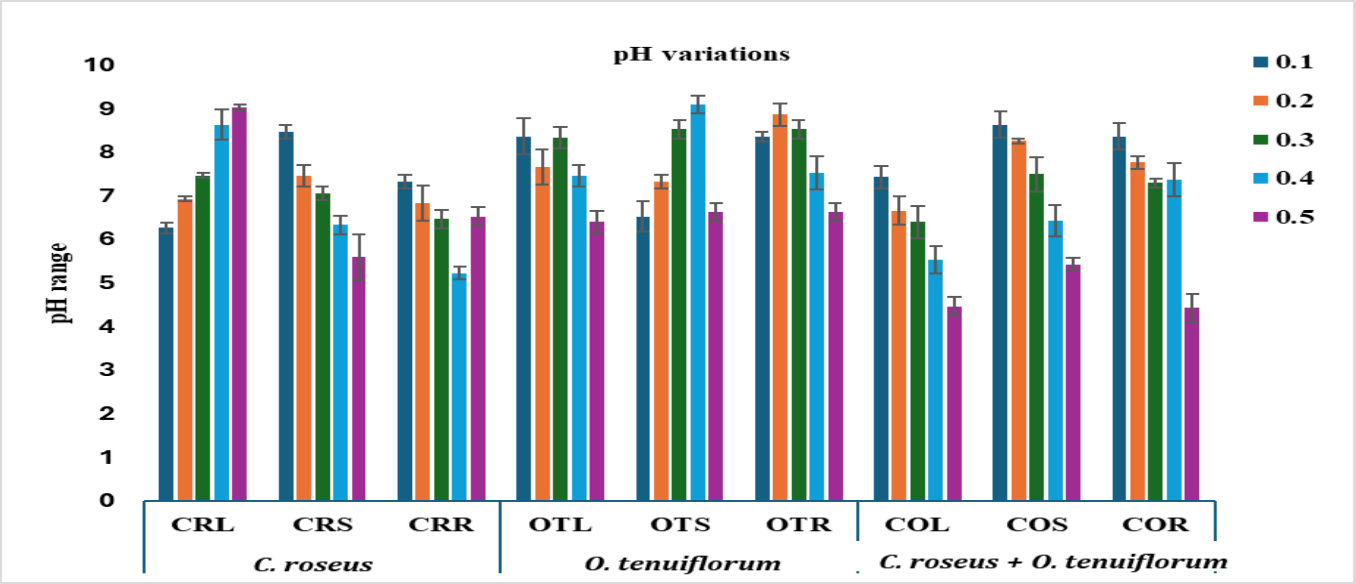

Fig. 1. Alterations in pH of wastewater after treatment with various coagulants.

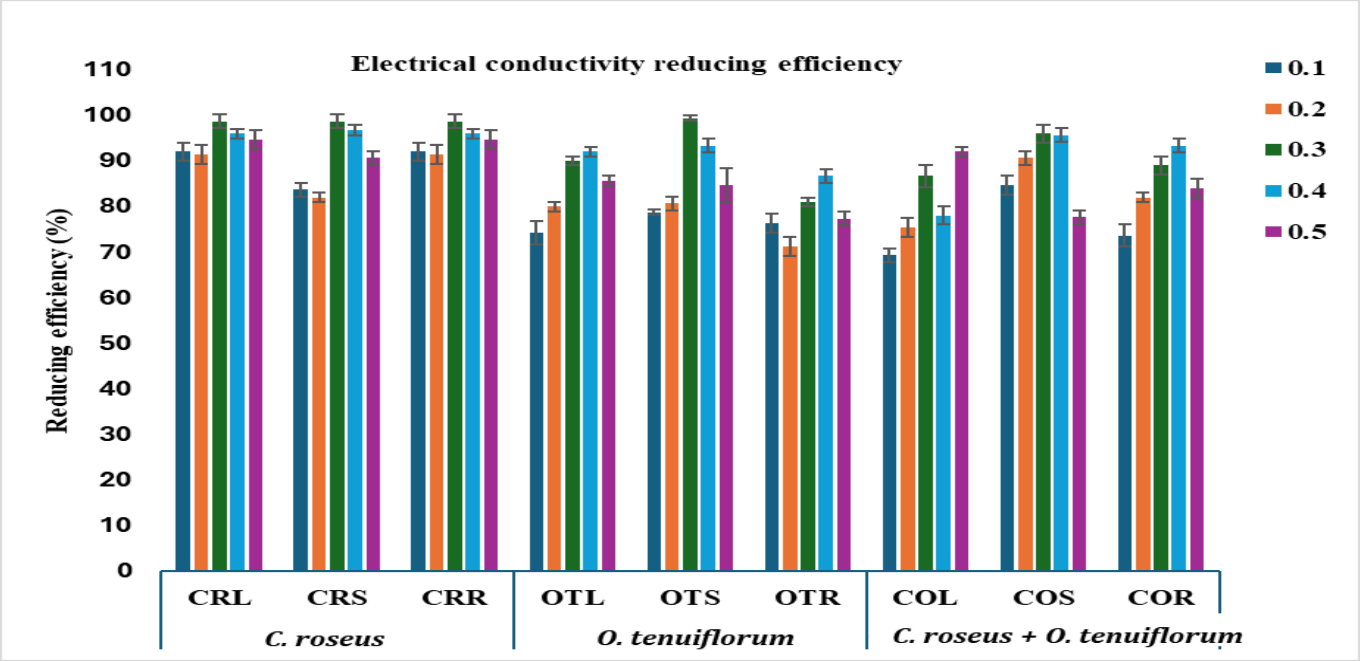

Fig. 2. Electrical conductivity (EC) reduces efficiency of all the coagulants.

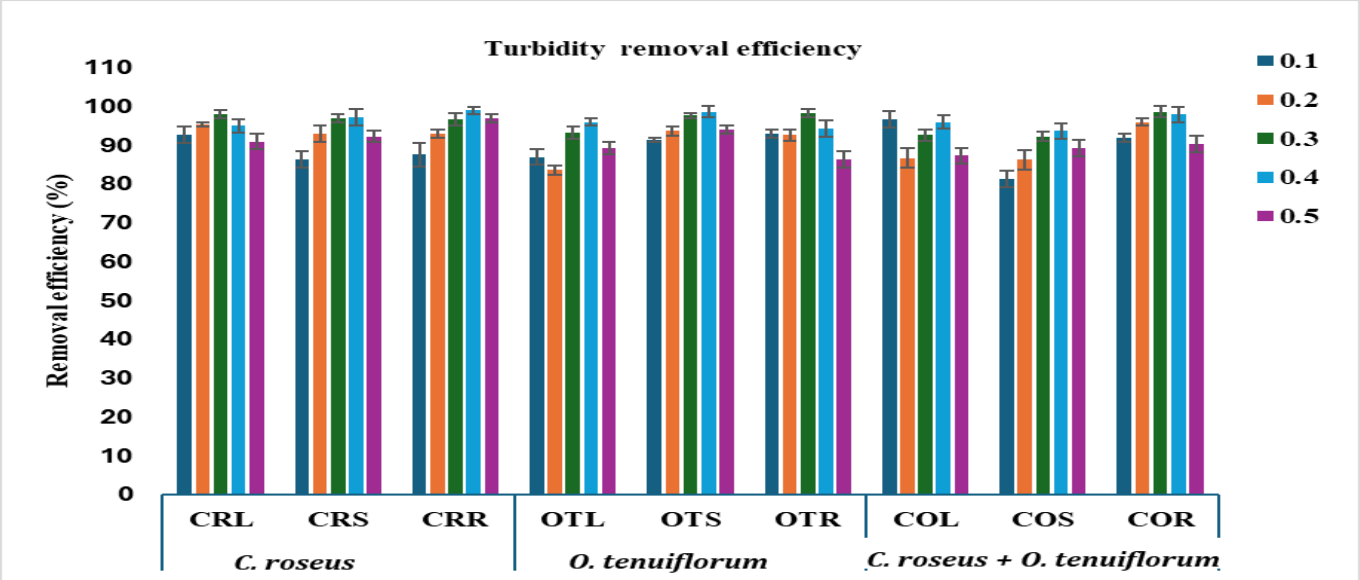

Fig. 3. Turbidity removal efficiency of all the coagulants.

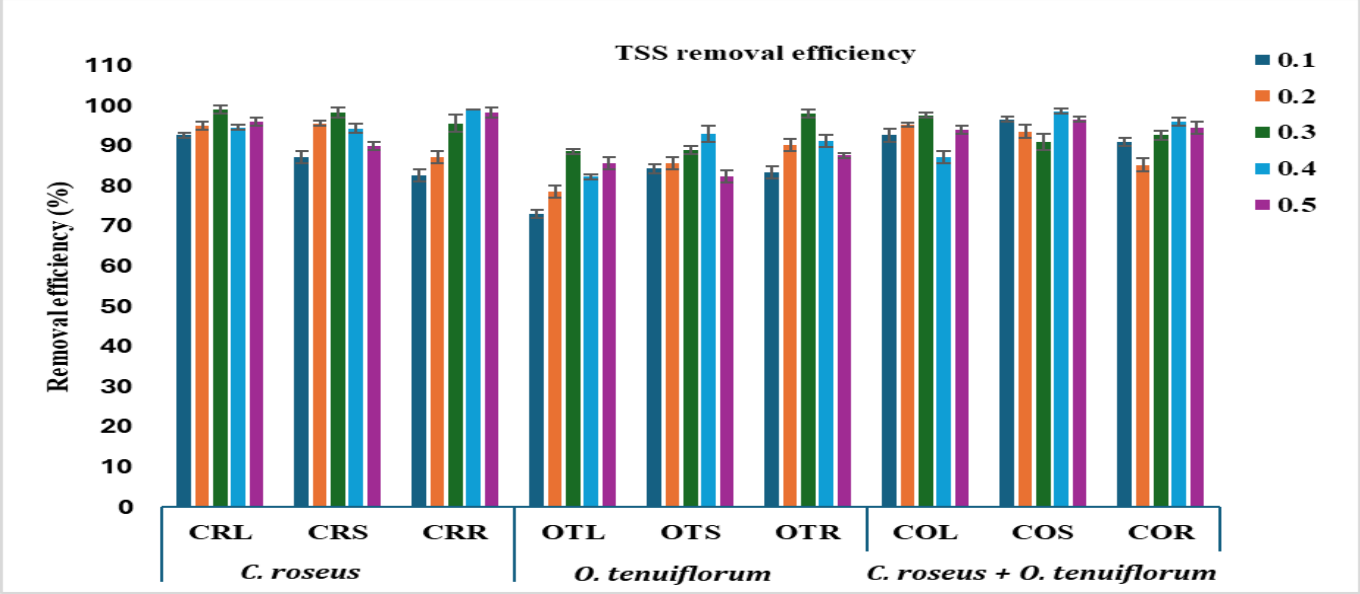

Fig. 4. Total suspended solids (TSS) removal efficiency of all coagulants.

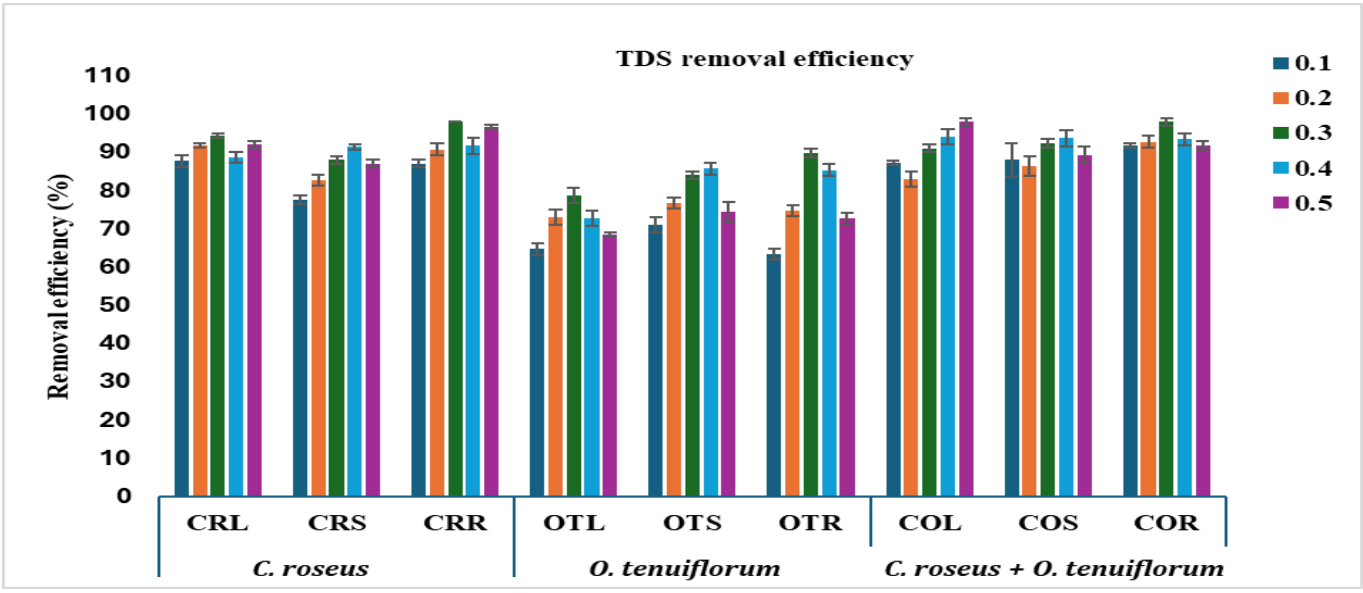

Fig. 5. Total dissolved solids (TDS) removal efficiency of all coagulants.

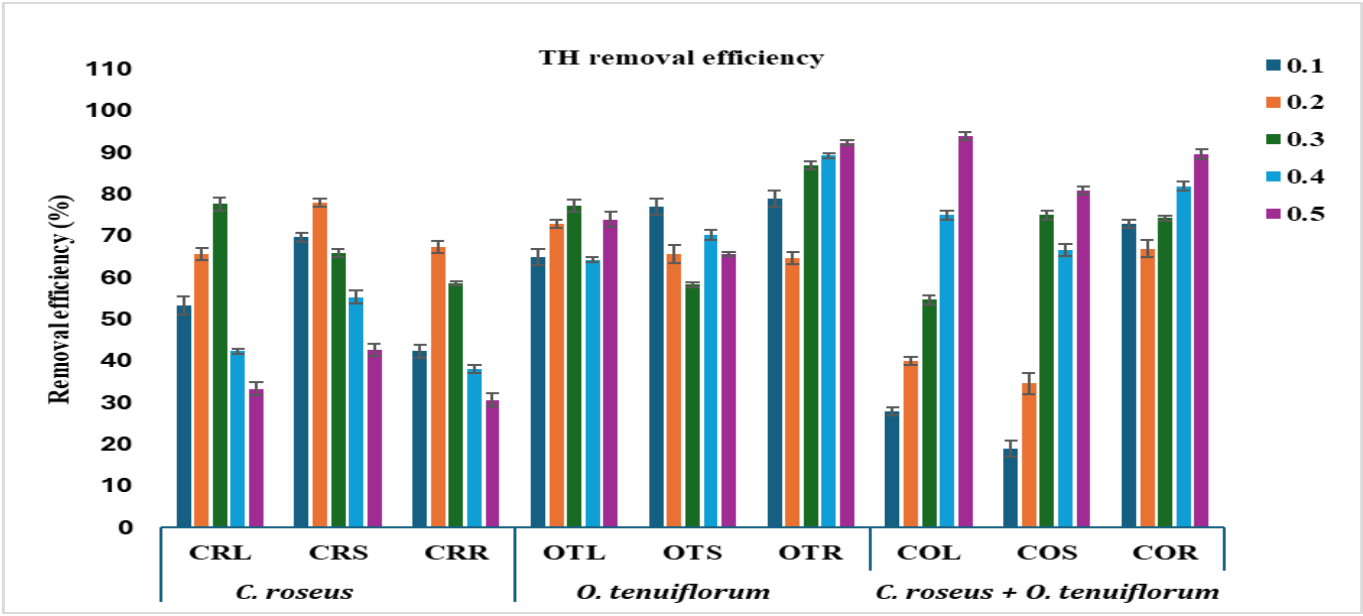

Fig. 6. Total hardness (TH) removal efficiency of all coagulants.

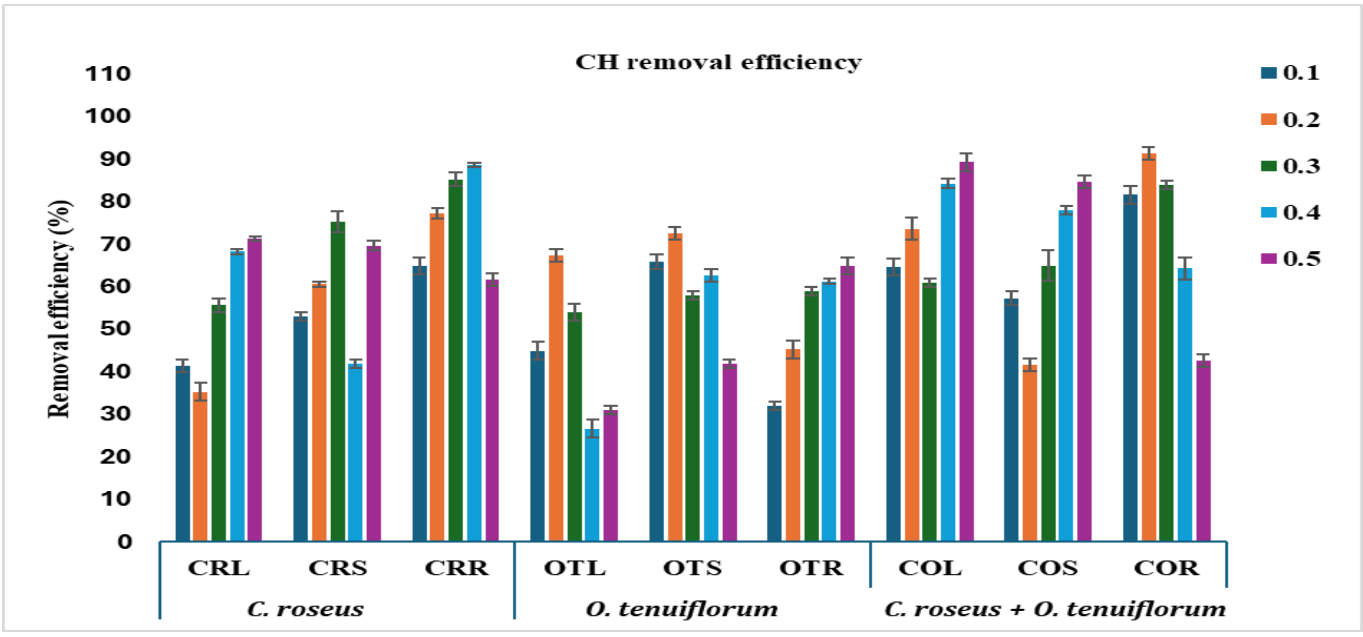

Fig. 7. Calcium hardness (CH) removal efficiency of all coagulants.

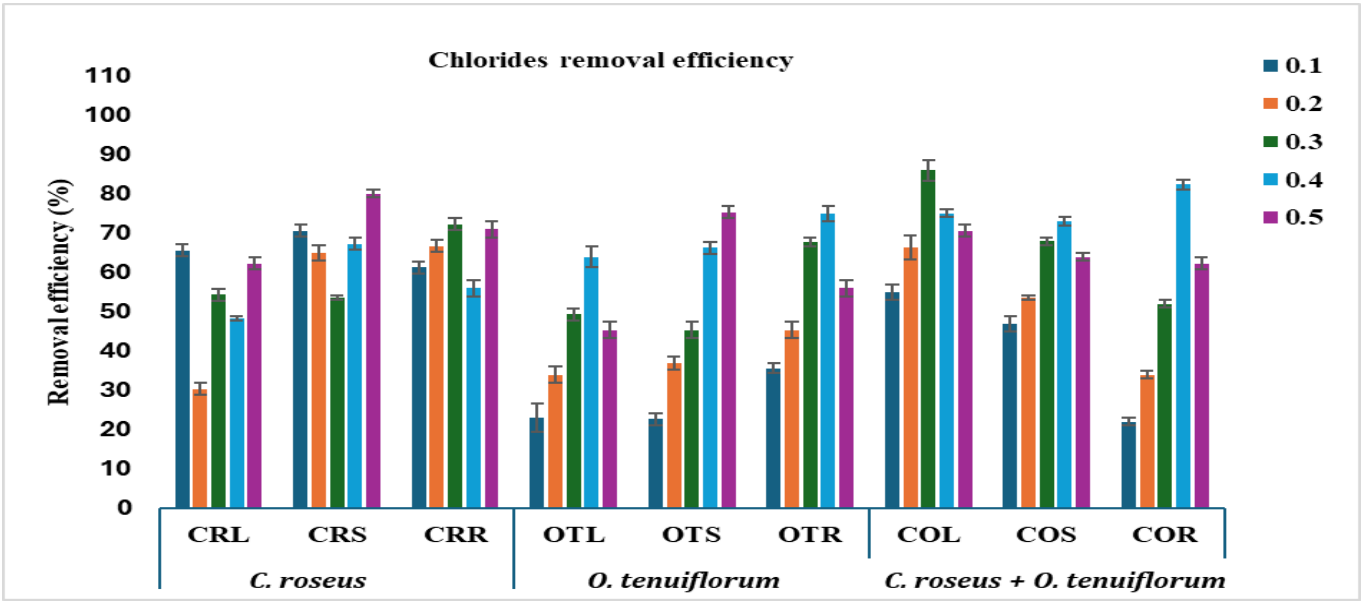

Fig. 8. Chlorides removal efficiency of all coagulants.

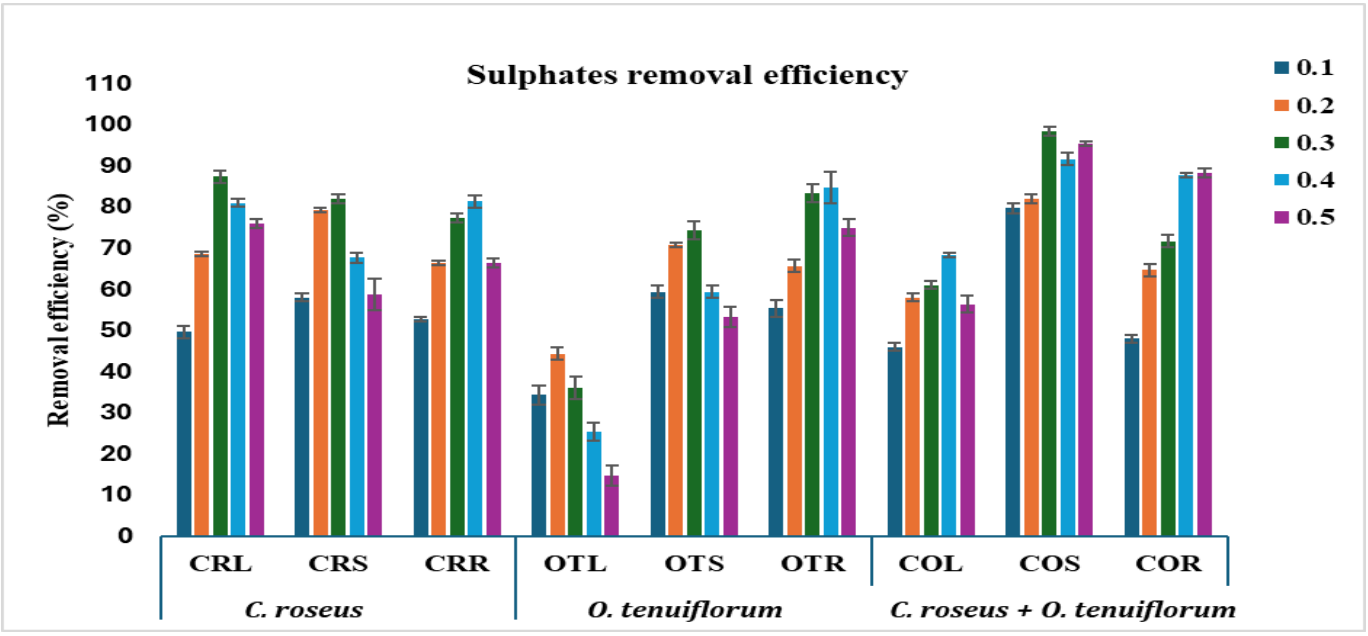

Fig. 9. Sulphates removal efficiency of all coagulants.

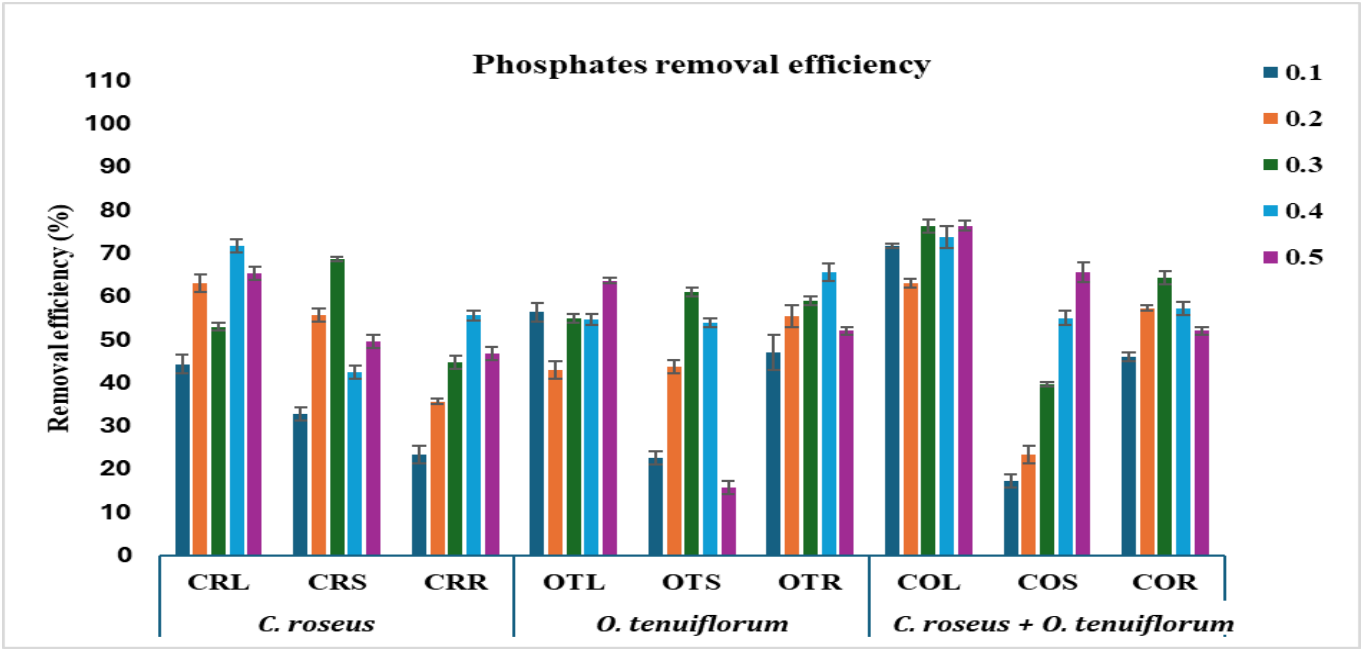

Fig. 10. Phosphates removal efficiency of all coagulants.

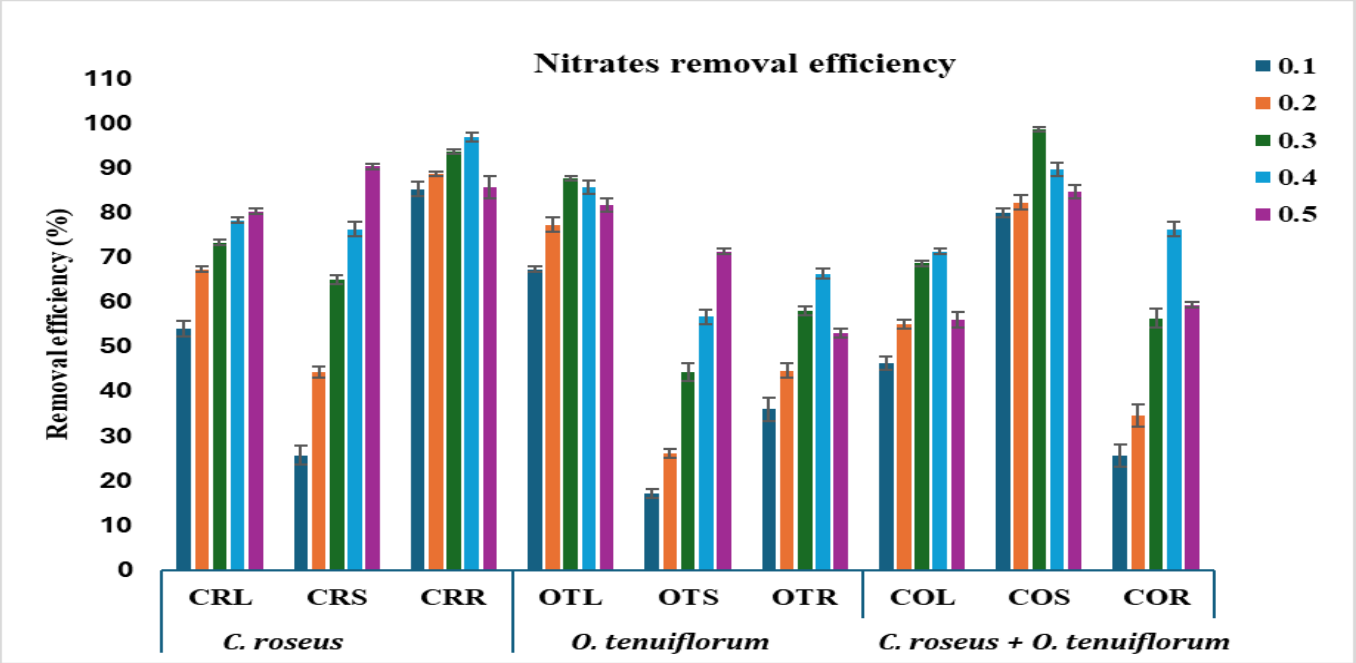

Fig. 11. Nitrates removal efficiency of all coagulants.

indicating that higher doses are required for the removal of hardness.

Various studies have reported that both chemical coagulants and bio-coagulants can effectively treat hardness in wastewater. A few studies carried out on *M. oleifera* seeds documented varying hardness removal efficiencies, with 0 to 15 % at an optimal dose of 125 mg/L and 23 to 34 % with a 50 mg/L dose (30). Some studies where the total hardness removal for *Moringa* seeds is negative, implying the coagulant failed to decrease the wastewater hardness. Ferric chloride, a chemical coagulant, showed negative removal for total hardness; however, calcium hardness removal was as high as 84.62 % at very minimal doses of 0.1 and 0.2 mg/L.

Chlorides, sulphates, phosphates and nitrates removal

Chloride removal using the coagulants to treat wastewater was analyzed as shown in Fig. 8. Chloride removal efficiency of 82.3 % was achieved with COR at a dosage of 0.4 g/l. Chemical coagulants such as alum, as a mixture with chitin, achieved the highest chloride reduction of 85.71 % at pH 7 and the bio-coagulant, chitin, exhibited maximum removal competence of 83.6 % at pH 7 (16). Chemical coagulant of ferric chloride showed the least chloride reduction of 36.46 %, while blended coagulants achieved the highest at 94-95 % (9).

Fig. 9 provides the analysis data for the removal efficiency of sulphates. Blend of *C. roseus* and *O. tenuiflorum* stems (COS) was able to efficiently clean up to 91 - 98.3 % of sulphates from the aquaculture wastewater at a minimal dosage range of 0.3 - 0.5 g/L. Other coagulants like CRL and OTR were able to degrade to 81 and 87 % at dosages of 0.4 - 0.5 g/L (9).

Phosphates removal

In terms of phosphate removal for aquaculture wastewater, the findings were presented in Fig. 10. The removal of phosphates was lower compared to the previous results of chlorides and sulphates. The highest removal efficiency was achieved by COL at a dose of 0.3, 0.4 and 0.5 g/L with an efficiency of 76.3, 73.6 and 76.3 %. It is evident from these results that the dosage for COL can be optimized to 0.3 g/L, as higher dosages of 0.4 g/L and 0.5 g/L exhibit similar efficiency. A study conducted on phosphate reduction in domestic wastewater using *Opuntia* and pomegranate peels revealed removal efficiencies of 90.32 and 89.03 % (31). Other studies carried out on *Carica* papaya seeds and *Moringa* seeds mixed with cactus powder also displayed higher phosphate removal efficiencies of 68.4 and 99.4 % (32).

Nitrates removal

Fig. 11 indicated that nitrate removal was higher for COS with 98.67 % efficiency at a dosage of 0.3 g/L, followed by CRR with 97 and 93.67 % removal capabilities at 0.4 and 0.3 g/L dosages, respectively. A similar trend was observed with chitosan hydrogel beads that exhibited a nitrate adsorption capacity of 92.1 mg/L at a dose of 1 g/L within 10 hrs (33). Various other studies on nitrate removal employing natural and chemical coagulants have also been conducted for treating wastewater via coagulation-flocculation. In a study conducted using chemical coagulants, ferric chloride achieved 90 % removal for nitrate concentrations up to 30 mg/L, which dropped to less than 35 % efficiency for higher concentrations of 70 mg/L (34). Alum had negligible removal capability even for low nitrate concentrations of up to 30 mg/L at a dose of 3.5-4 mg/L. Plant coagulants like *Moringa,* as a blend with cactus, exhibited nitrate removal with 90 % efficiency at a dose of 1.4 g/L, *Oputina* with 93.82 % efficiency and pomegranate peel was able to adsorb 3.71 mg/L of nitrates (9, 30). This signifies that CRR and COS have great potential to remove nitrates and can be used for treating aquaculture and other wastewaters with nitrate pollution.

Surface morphology analysis of bio-coagulants

Scanning Electron Microscope (SEM) micrography is mainly used for characterizing the morphology and structural changes of the bio-coagulants before and after the coagulation process. The SEM micrographs of the studied coagulants are presented in Fig. 12-14.

***Catharanthus roseus* coagulants - SEM analysis**

Fig. 12 (A, B) shows SEM images of the leaf surface before and after coagulation. The untreated leaf (A) architecture is characterized by coil-like hollow structures, indicating the presence of internal voids

Before coagulation

After coagulation

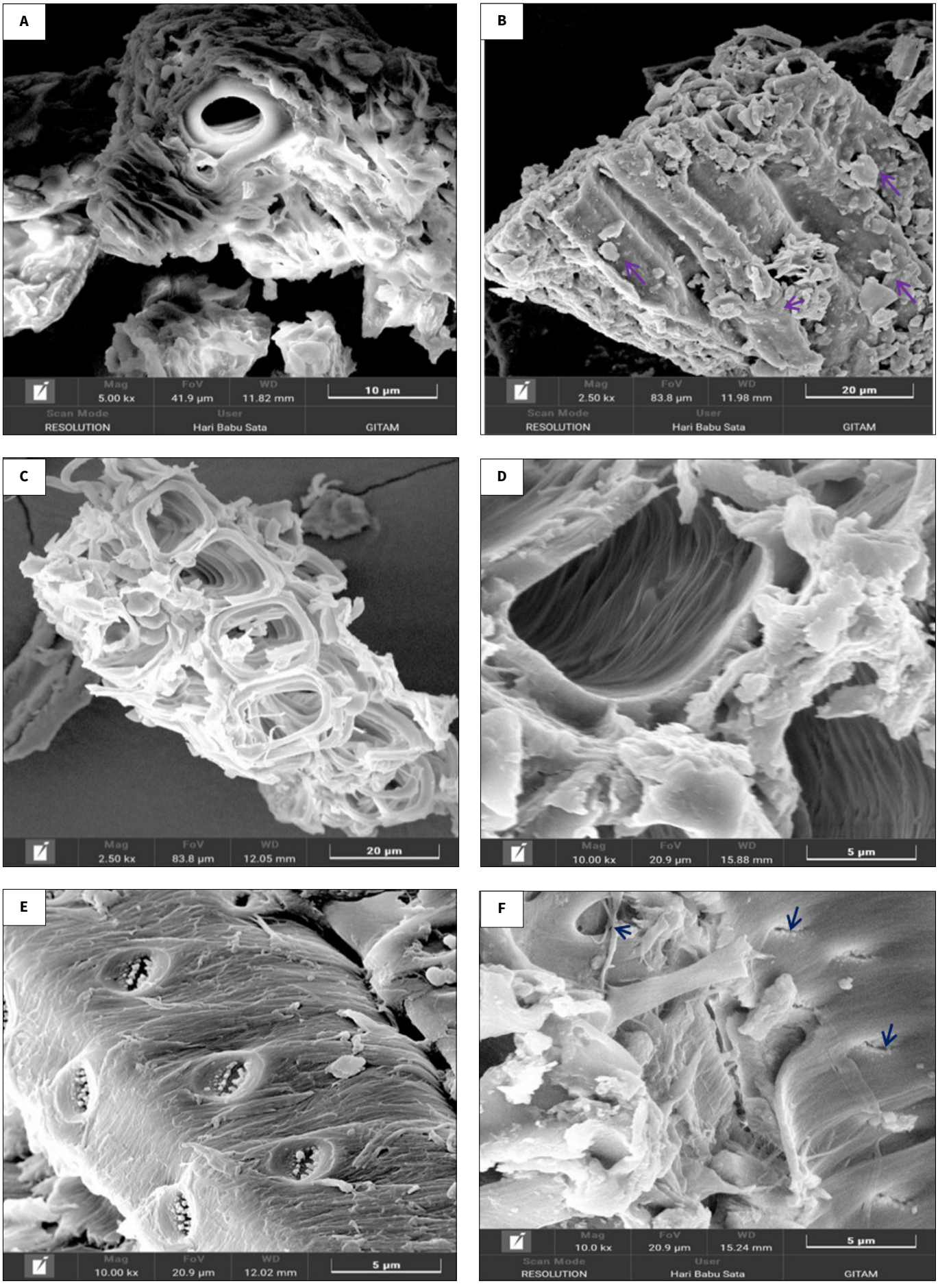

Fig. 12. SEM micrographs of *C. roseus* leaf (A and B), stem (C and D) and root (E and F). The left images are before coagulation and the right images are after coagulation.

Before coagulation

After coagulation

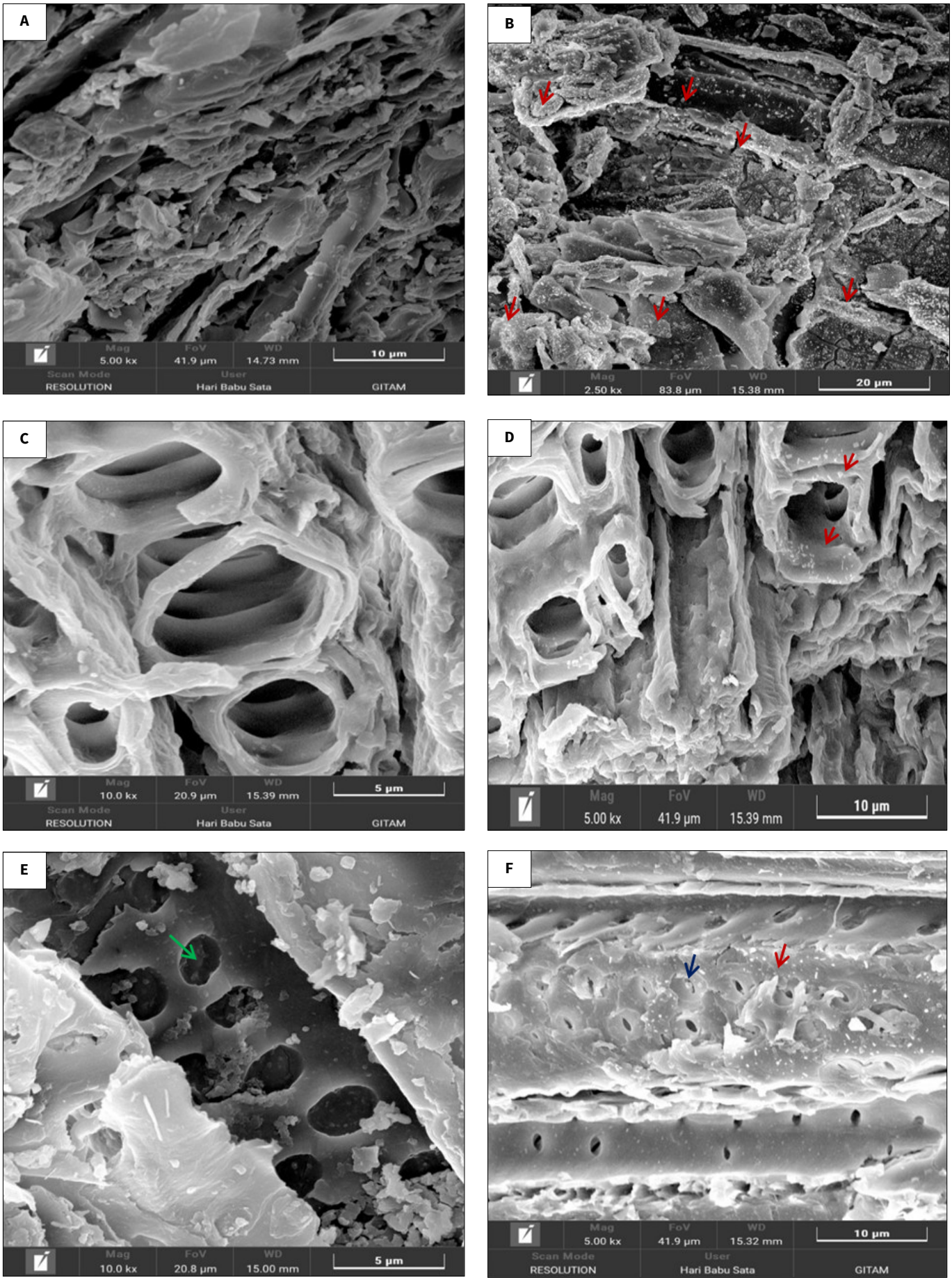

Fig. 13. SEM micrographs of *O. tenuiflorum* leaf (A and B), stem (C and D) and root (E and F). The left images are before coagulation and the right images are after coagulation.

Before coagulation

After coagulation

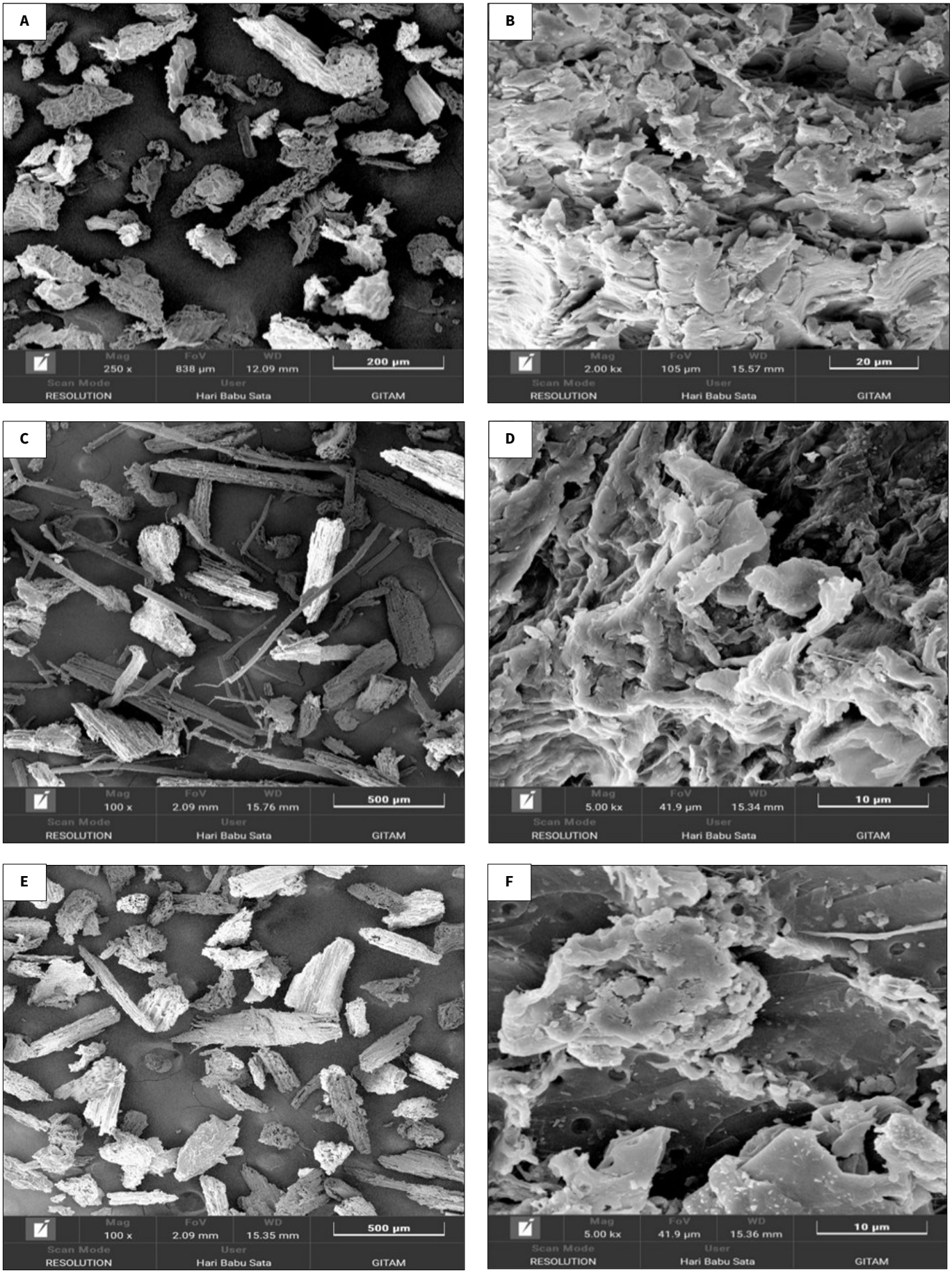

Fig. 14. SEM micrographs of *C. roseus* and *O. tenuiflorum* blend leaf (A and B), stem (C and D) and root (E and F). The left images are before coagulation and the right images are after coagulation.

that facilitate effective adsorption of pollutants (35). After coagulation (B), localized floc formation is observed on the coagulant surface (green arrows), suggestive of a surface adsorption mechanism. Fig. 12 (C, D) displays the stem structure. The pre-coagulation image (C) shows stacked, twisted ring structures, providing ample space for the adsorption of pollutants. Post-coagulation (D), a dense, compact layer of pollutants coats the surface, indicative of a surface complexation mechanism, characterized by strong binding of pollutants to functional groups. Fig. 12 (E, F) illustrates the root surface. In the untreated sample (E), rough, tubular structures with prominent tooth-like hollow cavities are observed. Following coagulation (F), these cavities are clogged with particulate matter (blue arrows), indicating a pore entrapment mechanism, where pollutants are physically retained within the porous structure.

In a study carried out on the use of *Picralima nitida* seeds as effective bio-coagulants for purification of aquaculture effluents, high heterogeneity on the seeds' surface, along with the existence of rough and irregular granular structures suggested the presence of active adsorption sites on its surface, contributing to its increased adsorption capability (28). In our studies, SEM images of *C. roseus* displayed heterogeneity and hollow structures contributing to enhanced adsorption and floc formation.

Ocimum tenuiflorum coagulants - SEM analysis

Scanning electron microscope (SEM) micrographs of *O. tenuiflorum* leaf, stem and root before and after coagulation experiments are shown in Fig. 13 (A-F). In Fig. 13 (A), leaf micrographs exhibit an uneven, rough and ridged morphology resembling folded sheets, providing multiple binding sites to capture pollutants (36). Treated leaf micrograph (B) shows a uniform distribution of fine particles, indicative of a surface adsorption mechanism via charge neutralization, where the positive charge of the coagulant neutralizes the negative charge of the pollutants, limiting repulsion and encouraging adhesion. Pre-coagulation SEM image of stem (C) reveals continuous, ring-like structures with significant hollow spaces. In the post-coagulation image (D), adsorption of pollutants is evident on the surface, supporting the occurrence of surface adsorption and complexation mechanisms. The untreated root micrograph (E) displays a prominent hollow tubular structure with evenly spaced circular holes all over the root, ideal for pollutant entrapment. The treated root image (F) shows pores clogged with particulate matter (blue arrows) and evenly dispersed pollutants on the surface (red arrows), suggesting a combinatorial mechanism of pore entrapment and surface adsorption.

Scanning electron microscope (SEM) images of *Ricinodendron rautanenii* seed grains used for treating turbidity in wastewater showed rough, irregularly shaped structures, an important feature required for good coagulant with respect to adsorption and bridging of colloidal particles (37). Similar patterns of rough and ridged morphology contributing to efficient adsorption and coagulation processes were visible in our studies providing strong support to the findings.

Blend of _C. roseus_ and _O. tenuiflorum_ coagulants - SEM analysis

To enhance pollutant removal efficiency, the above-studied plant-based coagulants were combined in a 1:1 ratio and applied to wastewater treatment. The SEM images of the leaf, stem and root of these coagulants before and after treatment are presented in Fig. 14 (A-F). The untreated images (A, C, E) reveal loosely arranged, unbound coagulant structures. The treated micrographs (B and D) show smooth, shiny surface layers, mainly the leaf and stem surfaces, suggesting the removal of oily organic matter via hydrophobic interactions. These regions often appear less with visible smear-like features rather than discrete particulate deposits. In contrast, the root micrograph (F) after treatment exhibits large, sponge-like agglomerates, a characteristic of the bridge flocculation mechanism. Post-coagulation shows a bridging mechanism where pollutants aggregate to form bigger flocs resembling sponge-like structures. This is mainly attributed to the bridging of high-molecular -weight biopolymers with several pollutant particles, causing large lumps or flocs.

Scanning electron microscope (SEM) images of a blend of *M. oleifera* and chitin used for cleaning wastewater displayed firm and dense structures after treatment indicating the adsorption of all impurities onto the surface (9). A similar dense matrix on the surface of *C. roseus* and *O. tenuiflorum* bi-blend were found correlating with the previous observation (Fig.14E, F).

Fourier transform infrared analysis of bio-coagulants

Fourier transform infrared spectral analysis was performed to study the various functional groups present in the bio-coagulants that contribute to the adsorption and treatment of pollutants in aquaculture wastewater. Fig. 15-17 present the FTIR spectra of leaf, stem and root coagulants of *C. roseus, O. tenuiflorum* and a blend of both coagulants. Analysis of the FTIR spectra is presented in Table 2-4.

The FTIR analysis of the respective spectra is depicted in Table 2-4, showing common peaks at 3272, 2921, 2852, 1617, 1414, 1243 and 1019 cm^{-1} for all the bio-coagulants in this study. The presence of abundant hydroxyl groups represented by the band at 3450 cm^{-1}, along with cellulose in coagulants, is attributed to their pollutant removal ability through adsorption. Similar findings have been observed in the study of neem leaves, orange peels, tamarind seeds and papaya seeds, where functional groups like hydroxyl (-OH), carboxylic acid (-COOH) and amines ($-NH_2$) were observed on the coagulants (38). Fourier transform infrared spectral analysis conducted on the *Sesamum indicum* biopolymers used for removing TDS from wastewater also showed N-H stretching, carboxyl group, hydroxyl group and amide groups (39).

The peak at 3292 cm^{-1} indicates the presence of carboxylic acid groups, contributing to charge neutralization or electrostatic interactions in both *Catharanthus* and *Ocimum* (Fig. 15-17). O-H stretching at the 3326 cm^{-1} peak and C-H stretching at the 2916 cm^{-1} peak result in Van der Waals forces, where initial floc formation takes place by weak interaction between the non-polar regions of the coagulant and pollutant.

This supports the SEM image observed for *C. roseus* root in Fig. 12 (B). The peak at 2921 cm^{-1} arises from asymmetric stretching of -CH (CH_2) vibration and the C=O stretching is linked to peaks in 1731 and 1617 cm^{-1}. All the specified coagulants in this study have peaks at 1731 and 1617 cm^{-1}, supporting their surface complexation mechanism, forming flocs on the surface as seen in SEM images, relating to the plant stem (Fig. 12D, 13D). Hydrogen bonding mainly takes place due to C-N stretching at 1012 cm^{-1}, indicating the presence of amines or protein in the coagulant (Fig. 16, 17). The peaks ranging from 700-600 cm^{-1} occur due to M-O stretch, where metal ion complexation takes place (Fig. 15-17).

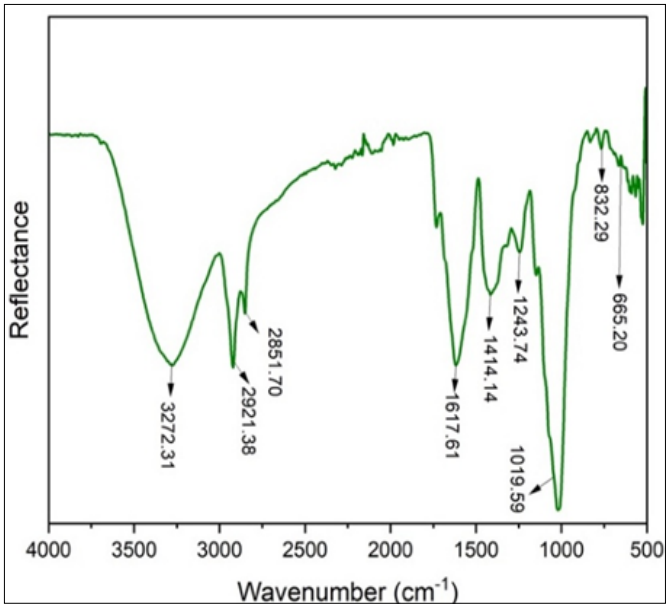

(A) *C. roseus* leaf (CRL)

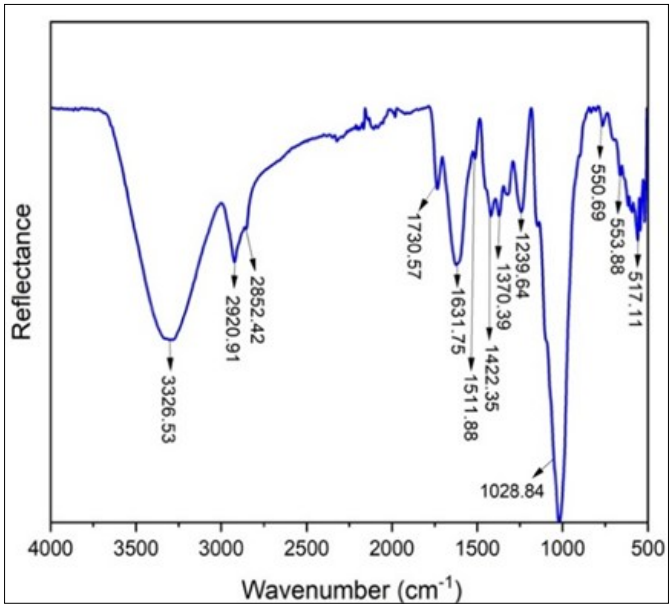

(B) *C. roseus* stem (CRS)

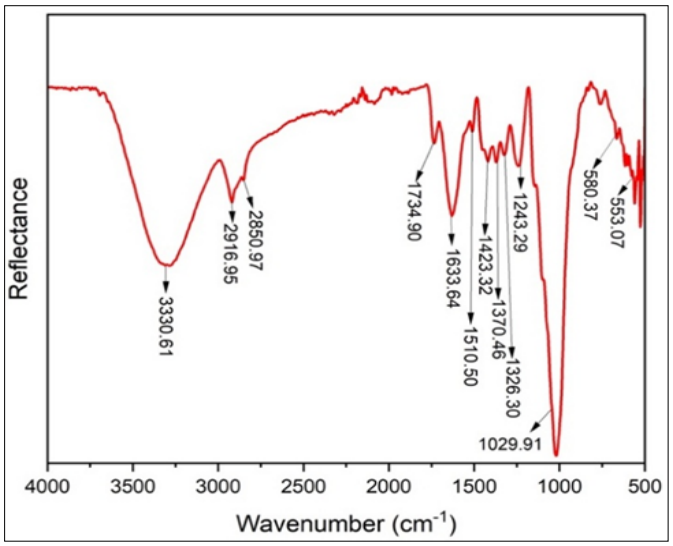

(C) *C. roseus* root (CRR)

Fig. 15. FTIR spectra of leaf (A), stem (B) and root (C) of *C. roseus.*

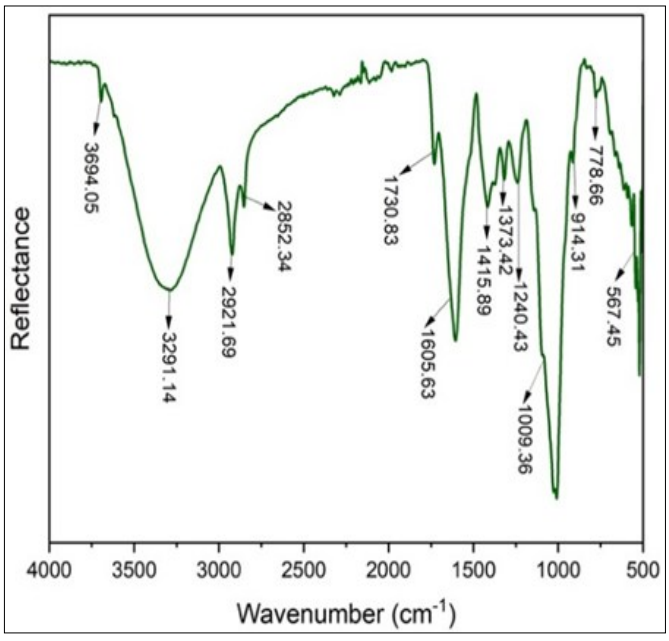

(A) *O. tenuiflorum* leaf (OTL)

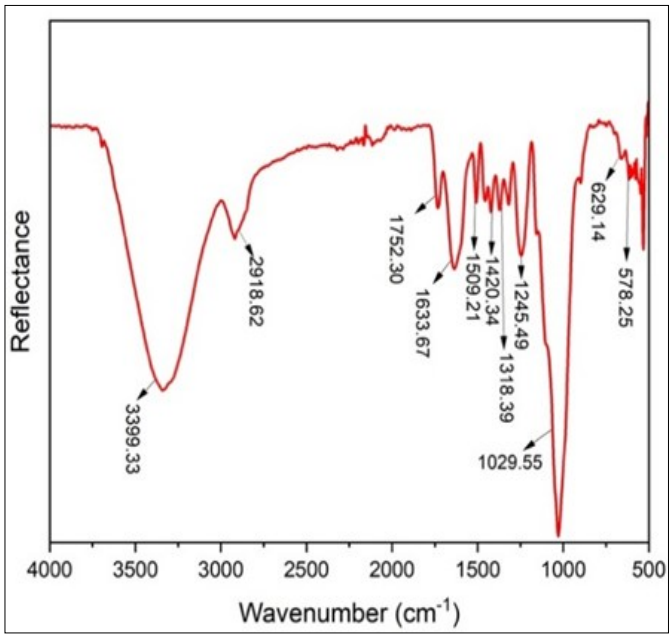

(B) *O. tenuiflorum* stem (OTL)

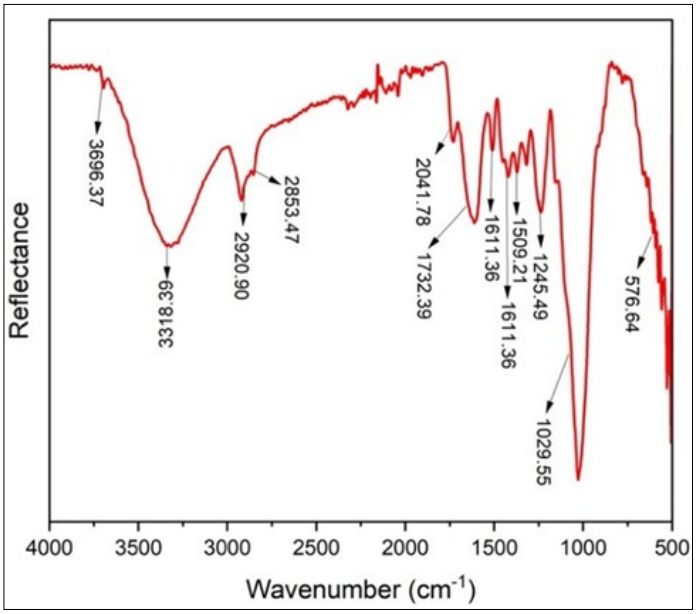

(C) *O. tenuiflorum* root (OTR)

Fig. 16. FTIR spectra of leaf (A), stem (B) and root (C) of *O. tenuiflorum.*

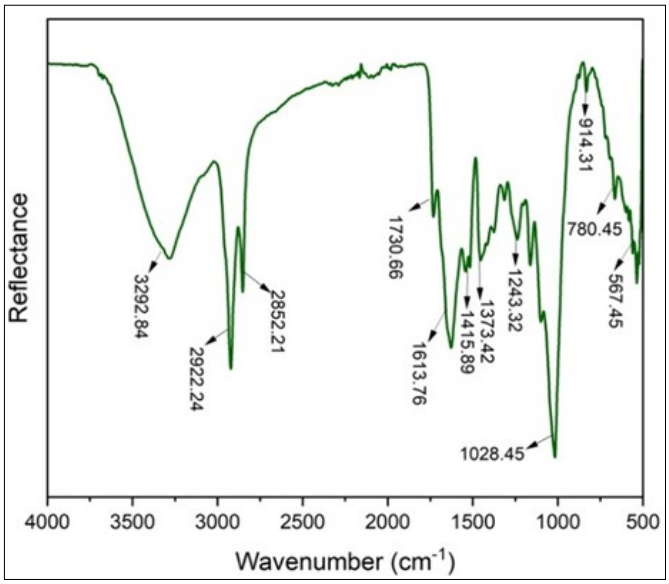

(A) Leaf blend

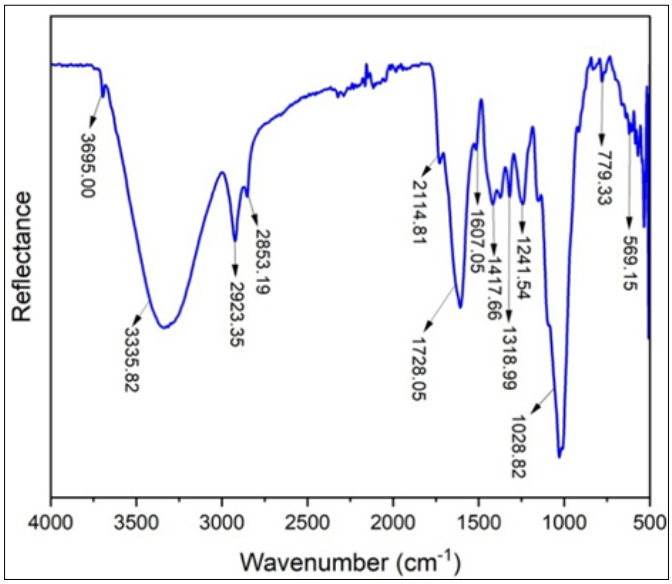

(B) Shoot blend

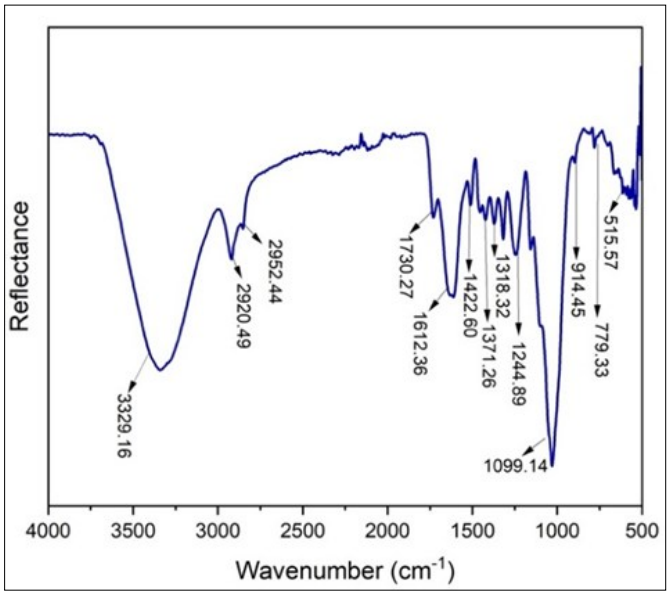

(C) Root blend

Fig. 17. FTIR spectra of leaf (A), stem (B) and root (C) of *C. roseus* and *O. tenuiflorum* blend.

Table 2. FTIR spectrum analysis of leaf, stem and root of *C. roseus*

Wave number (cm^{-1})			Functional group	Peak appearance	Class of the identified compound
Leaf	Stem	Root			
-	3326.53	3330.61	O-H stretching	Broad	Intermolecular bonded alcohol
3272.31	-	-	O-H stretching	Broad	Carboxylic acid
2921.38	2920.91	2916.95	C-H stretching	Narrow	Alkane
2851.72	2852.42	2852.18	C-H stretching	Narrow	Alkane
-	1730.57	1734.90	C=O stretching	Narrow	Aldehyde
-	1631.74	1633.84	C=O stretching	Medium	Amide
1617.61	-	-	C=C stretching	Medium	Ketone
-	1511.88	1510.50	N-O stretching	Medium	Nitro compound
1414.14	1422.35	1423.32	C-H bending	Medium	Alkane
-	1370.39	1370.46 1326.30	C-F stretching	Narrow	Fluoro compound
1243.74	1239.64	1243.29	C-N stretching	Medium	Amine
1019.59	1028.84	1029.91	C-O stretching	Narrow	Primary alcohol
-	560.69 538.89 517.11 507.37	580.37 557.08 533.07 515.94	M-O stretching	Narrow	Metal oxides

Table 3. FTIR spectrum analysis of leaf, stem and root of *O. tenuiflorum*

Wave number (cm^{-1})			Functional group	Peak appearance	Class of the identified compound
Leaf	Stem	Root			
3694.05	-	3696.37	O-H stretching	Medium	Free alcohol
-	3393.33	3318.39	O-H stretching	Broad	Intermolecular bonded alcohol
3291.14	-	-	O-H stretching	Broad	Carboxylic acid
2921.69	2918.62	2920.90	C-H stretching	Narrow	Alkane
2852.34	-	2853.47	C-H stretching	Narrow	Alkane
-	-	2041.78	C-H bending	Narrow	Aromatic compound
1730.83	1732.39	1729.65	C=O stretching	Narrow	Aldehyde
-	1636.69	-	C=O stretching	Narrow	Conjugated alkene
1605.63	-	1611.36	C=O stretching	Medium	Amide
-	1508.51	1509.21	N-O stretching	Medium	Nitro compound
1415.89 1419.27	1422.78	1420.34	C-H bending	Medium	Alkane
1373.42 1318.08	1371.72 1319.10	1318.39	C-F stretching	Narrow	Fluoro compound
1240.43	-	1237.64	C-N stretching	Medium	Amine
1009.36	1029.55	1028.21	C-O stretching	Narrow	Primary alcohol
914.31	-	-	NH-wag	Narrow	Primary and secondary amines
778.66	-	-	C-H bending	Narrow	1,2,3-trisubstituted Primary alcohol
-	659.14	-	C-Br stretching	Narrow	Halo compound
567.45	578.25	559.62	M-O stretching	Narrow	Metal oxides
544.50	548.01	529.39			
520.56	532.39	505.66			
505.66	514.85				

Table 4. FTIR spectrum analysis of leaf, stem and root blend of *C. roseus* and *O. tenuiflorum*

Wave number (cm^{-1})			Functional group	Peak appearance	Class of the identified compound
Leaf	Stem	Root			
-	3695.00	-	O-H stretching	Medium	Free alcohol
-	3335.82	3329.18	O-H stretching	Broad	Intermolecular bonded alcohol
3292.14	-	-	O-H stretching	Broad	Carboxylic acid
2922.64	2923.35	2920.46	C-H stretching	Narrow	Alkane
2852.21	2853.19	2852.44	C-H stretching	Narrow	Alkane
-	2114.81	-	C-H bending	Narrow	Aromatic compound
1730.66		1730.27	C-H stretching	Narrow	Aldehyde
1613.69	1607.05	1612.36	C=O stretching	Medium	Amide
1417.10	1417.66	1422.60	C-H bending	Medium	Alkane
1373.43	1374.06 1318.99		C-F stretching	Narrow	Fluoro compound
1243.32	1241.54	1244.89	C-N stretching	Medium	Amine
1150.63	-		C-S stretching	Narrow	Secondary alcohol
1028.45	1028.82	1099.14	C-O stretching	Narrow	Primary alcohol
-	914.45	-	NH-wag	Narrow	Primary and secondary amines
-	-	897.54	C-C stretching	Narrow	Alkenes
780.48	779.33	-	C-H bending	Narrow	1,2,3-trisubstituted Primary alcohol
-	619.96	-	C-Br stretching	Narrow	Halo compound
534.98	569.15	515.18	M-O stretching	Narrow	Metal oxides

According to a recent study conducted on the aquaculture effluent purification with *P. nitida* seeds, the FTIR spectral data showed N-H stretching corresponding to the presence of amino compounds, an indication of protein. The spectrum also revealed carboxyl groups (C=O), hydroxyl groups (O-H) and hydrogen bonding (28). The treatment of fish farm water with green coagulants like palm pith, watermelon rinds revealed FTIR spectra with functional groups of N-H, O-H, C-H, C-N stretching representing the crucial roles of these groups in coagulation-flocculation process (40). Recent studies performed on turbidity removal in water systems employing lupin beans and rice straw extracts showed peaks of hydroxyl groups, -CH stretching bands, C=O stretching, C-O stretching vibrations of ketones, aldehydes, lactones (41). All these studies provide strong evidence for our studies where similar findings were observed, indicating effective bio-coagulation process.

Conclusion

In this study, two underexplored medicinal plants -namely, *C. roseus* and *O. tenuiflorum* were tested to treat aquaculture wastewater. Our experimental findings demonstrated the significant potential of these natural coagulants in removing major pollutants from aquaculture wastewater, with overall efficiency observed at an optimal dose range of 0.3-0.4 g/L, offering a sustainable, low-cost and eco-friendly solution to aquaculture wastewater treatment. Future research can be aimed at developing standardized protocols for large-scale extraction, purification and stabilization of plant-based natural coagulants for application in commercial aquaculture operations. This study can also be expanded for screening of locally available indigenous and medicinal plants as natural coagulants for treating aquaculture wastewater.

Acknowledgements

The authors acknowledge Department of Life Science, School of Science, Gandhi Institute of Technology and Management (Deemed to be University), Visakhapatnam for providing institutional support to conduct the research. The authors also extend their sincere thanks to the MURTI-SAIF facility at GITAM University for providing access to the SEM and Dr. Harihara Padhy, Nanotechnology Lab, GITAM University, for providing support with ATR-FTIR analysis. The authors express their gratitude to Dr. Nageswara Rao, Rajkamal hatcheries, for providing the water samples.

Authors' contributions

CC and HM were responsible for execution of the experimental work and contributed to the writing of the manuscript. PK conceptualized and supervised the overall research. SV provided expert guidance and technical support throughout the study. All authors read and approved the final manuscript.

Compliance with ethical standards

Conflict of interest: Authors do not have any conflict of interests to declare.

Ethical issues: None

References

1. Garlock T, Asche F, Anderson J, Ceballos-Concha A, Love DC, Osmundsen TC, Pincinato RBM. Aquaculture: the missing contributor in the food security agenda. Glob Food Secur. 2022;32:100620. https://doi.org/10.1016/j.gfs.2022.100620
2. Singh BJ, Chakraborty A, Sehgal R. A systematic review of industrial wastewater management: evaluating challenges and enablers. J Environ Manage. 2023;348:119230. https://doi.org/10.1016/j.jenvman.2023.119230
3. Dauda AB, Ajadi A, Tola-Fabunmi AS, Akinwole AO. Waste production in aquaculture: sources, components and managements in different culture systems. Aquac Fish. 2019;4(3):81-8. https://doi.org/10.1016/j.aaf.2018.10.002
4. Iber BT, Kasan NA. Recent advances in shrimp aquaculture wastewater management. Heliyon. 2021;7(11):e08283. https://doi.org/10.1016/j.heliyon.2021.e08283
5. Gizaw A, Zewge F, Kumar A, Mekonnen A, Tesfaye M. A comprehensive review on nitrate and phosphate removal and recovery from aqueous solutions by adsorption. J Water Supply Res Technol-Aqua. 2021;70(7):921-47. https://doi.org/10.2166/aqua.2021.070
6. Ravindiran G, Rajamanickam S, Sivarethinamohan S, Karupaiya Sathaiah B, Ravindran G, Muniasamy SK, Hayder G. A review of the status, effects, prevention and remediation of groundwater contamination for sustainable environment. Water. 2023;15(20):3662. https://doi.org/10.3390/w15203662
7. Fraga-Corral M, Ronza P, Garcia-Oliveira P, Pereira AG, Losada AP, Prieto MA, et al. Aquaculture as a circular bio-economy model with Galicia as a study case: how to transform waste into revalorized by-products. Trends Food Sci Technol. 2022;119:23-35. https://doi.org/10.1016/j.tifs.2021.10.022
8. El-taweel RM, Mohamed N, Alrefaey KA, Husien S, Abdel-Aziz AB, Salim AI, et al. A review of coagulation explaining its definition, mechanism, coagulant types and optimization models; RSM and ANN. Curr Res Green Sustain Chem. 2023;6:100358. https://doi.org/10.1016/j.crgsc.2023.100358
9. Karnena MK, Konni M, Dwarapureddi BK, Saritha V. Blend of natural coagulants as a sustainable solution for challenges of pollution from aquaculture wastewater. Appl Water Sci. 2022;12(3):47. https://doi.org/10.1007/s13201-022-01563-5
10. Karnena MK, Saritha V. Contemplations and investigations on green coagulants in treatment of surface water: a critical review. Appl Water Sci. 2022;12(7):150. https://doi.org/10.1007/s13201-022-01641-8
11. Kumar Karnena M, Saritha V. Phytochemical and physicochemical screening of plant-based materials as coagulants for turbidity removal - an unprecedented approach. Watershed Ecol Environ. 2022;4:188-201. https://doi.org/10.1016/j.wsee.2022.07.002
12. Soumya V, Kiranmayi P. Potential of *Catharanthus roseus* applied to remediation of disparate industrial soils owing to accumulation and translocation of metals into plant parts. Int J Phytoremediation. 2023;25(6):746-58. https://doi.org/10.1080/15226514.2022.2146001
13. Soumya V, Sowjanya A, Kiranmayi P. Evaluating the status of phytochemicals within *Catharanthus roseus* due to higher metal stress. Int J Phytoremediation. 2021;23:1-11. https://doi.org/10.1080/15226514.2020.1863287
14. Hira FA, Islam A, Mitra K, Bithi UH, Ahmed KS, Islam S, et al. Comparative analysis of phytochemicals and antioxidant characterization among different parts of *Catharanthus roseus*: *In vitro* and *in silico* investigation. Biochem Res Int. 2024;2024:1904029. https://doi.org/10.1155/2024/1904029
15. Qamar F, Sana A, Naveed S, Faizi S. Phytochemical characterization, antioxidant activity and antihypertensive evaluation of *Ocimum basilicum* L. in l-NAME induced hypertensive rats and its correlation

analysis. Heliyon. 2023;9(4):e14644. https://doi.org/10.1016/j.heliyon.2023.e14644

16. Vara S. Screening and evaluation of innate coagulants for water treatment: a sustainable approach. Int J Energy Environ Eng. 2012;3(1):29. https://doi.org/10.1186/2251-6832-3-29
17. Saritha V, Karnena MK, Dwarapureddi BK. Exploring natural coagulants as impending alternatives towards sustainable water clarification– a comparative studies of natural coagulants with alum. J Water Process Eng. 2019;32:100982. https://doi.org/10.1016/j.jwpe.2019.100982
18. Adjovu GE, Stephen H, James D, Ahmad S. Measurement of total dissolved solids and total suspended solids in water systems: a review of the issues, conventional and remote sensing techniques. Remote Sens. 2023;15(14):3534. https://doi.org/10.3390/rs15143534
19. Rice EW, Baird RB, Eaton AD, Clesceri LS. Standard methods for the examination of water and wastewater. 22nd ed. APHA 2016, Washington DC.
20. Diver D, Nhapi I, Ruziwa WR. The potential and constraints of replacing conventional chemical coagulants with natural plant extracts in water and wastewater treatment. Environ Adv. 2023;13:100421. https://doi.org/10.1016/j.envadv.2023.100421
21. Saritha V, Karnena MK, Dwarapureddi BK. Competence of blended coagulants for surface water treatment. Appl Water Sci. 2020;10(1):20. https://doi.org/10.1007/s13201-019-1102-4
22. Rasheed FA, Alkaradaghi K, Al-Ansari N. The potential of *Moringa oleifera* seed in water coagulation-flocculation technique to reduce water turbidity. Water Air Soil Pollut. 2023;234(4):250. https://doi.org/10.1007/s11270-023-06132-3
23. Shahzadi F, Haydar S, Tabraiz S. Optimization of coagulation to remove turbidity from surface water using novel nature-based plant coagulant and response surface methodology. Sustainability. 2024;16(7):2941. https://doi.org/10.3390/su16072941
24. Bahrodin MB, Zaidi NS, Kadier A, Hussein N, Syafiuddin A, Boopathy R. A novel natural active coagulant agent extracted from the sugarcane bagasse for wastewater treatment. Appl Sci. 2022;12(16):7972. https://doi.org/10.3390/app12167972
25. Hussain G, Haydar S. Comparative evaluation of *Glycine max* L. and alum for turbid water treatment. Water Air Soil Pollut. 2020;231(2):57. https://doi.org/10.1007/s11270-020-4427-3
26. Unnisa SA, Bi SZ. *Carica papaya* seeds effectiveness as coagulant and solar disinfection in removal of turbidity and coliforms. Appl Water Sci. 2018;8(6):149. https://doi.org/10.1007/s13201-018-0781-4
27. Ahmad A, Abdullah SRS, Hasan HA, Othman AR, Kurniawan SB. Aquaculture wastewater treatment using plant-based coagulants: evaluating removal efficiency through the coagulation-flocculation process. Results Chem. 2024;7:101390. https://doi.org/10.1016/j.rechem.2024.101390
28. Igwegbe CA, Ovuoraye PE, Białowiec A, Okpala COR, Onukwuli OD, Dehghani MH. Purification of aquaculture effluent using *Picralima nitida* seeds. Sci Rep. 2022;12(1):21594. https://doi.org/10.1038/s41598-022-25872-1
29. Geresu BA, Ebba M. Investigations on the removal of phosphate and nitrate using a mixture of cactus and moringa seed powder via RSM techniques. Desalination Water Treat. 2024;320:100856. https://doi.org/10.1016/j.desal.2024.100856
30. Lwasa A, Mdee OJ, Ntalikwa JW, Sadiki N. Performance analysis of plant-based coagulants in water purification: a review. Discov Water. 2024;4(1):108. https://doi.org/10.1007/s43832-024-00108-6
31. Ahmed Hussein M, El-Khateeb Mohamed A, Mohamed NY, Sobhy NA, Fawzy ME. Evaluation of different natural waste materials as bio-coagulants for domestic wastewater treatment. Desalination Water Treat. 2024;317:100034. https://doi.org/10.1016/j.desal.2024.100034
32. Vezar SAN, Belinda ZT, Rendana M, Agustina TE, Nasir S, Hanum L, Andarini D. The use of *Carica papaya* seeds as bio coagulant for laundry wastewater treatment. J Eng Appl Sci. 2024;71(1):99.
33. Chatterjee S, Woo SH. The removal of nitrate from aqueous solutions by chitosan hydrogel beads. J Hazard Mater. 2009;164(2-3):1012-18. https://doi.org/10.1016/j.jhazmat.2008.09.020
34. Aghapour AA, Nemati S, Mohammadi A, Nourmoradi H, Karimzadeh S. Nitrate removal from water using alum and ferric chloride: a comparative study of alum and ferric chloride efficiency. Environ Health Eng Manag. 2016;3(2):69-73.
35. Soumya V, Kiranmayi P, Siva Kumar K. Morpho-anatomical responses of *Catharanthus roseus* due to combined heavy metal stress observed under scanning electron microscope. Plant Sci Today. 2022.9(3):623-31. https://doi.org/10.14719/pst.1621
36. Kurniawan S, Ahmad A, Imron M, Abdullah SRS, Abu Hasan H, Othman AR, Kuncoro EP. Performance of chemical-based vs bio-based coagulants in treating aquaculture wastewater and cost-benefit analysis. Pol J Environ Stud. 2023;32(2):1177-87. https://doi.org/10.15244/pjoes/153390
37. Namane PI, Letshwenyo MW, Yahya A. Evaluation of plant-based coagulants for turbidity removal and coagulant dosage prediction using machine learning. Environ Technol. 2025;46(14):2570-85. https://doi.org/10.1080/09593330.2023.2291456
38. Rawat DR, Parmar KM, Thorat SS. Comparative analysis of plant-based natural coagulants for wastewater treatment. Curr World Environ. 2025;20(1):395-409.
39. Igwegbe CA, Onukwuli OD. Removal of total dissolved solids (TDS) from aquaculture wastewater by coagulation-flocculation process using *Sesamum indicum* extract: effect of operating parameters and coagulation-flocculation kinetics. The Pharm Chem J. 2019;6(4):32-45.
40. Al-Baldawi IA, Hussain A. Nutrient fate after the coagulation-flocculation process of fish-farm water using green coagulant. J Ecol Eng. 2025;26(5):65-72. https://doi.org/10.12911/22998993/184250
41. Amin NK, Abdelwahab O, El-Ashtoukhy ESZ, Abdel-Aziz MH. Comparative analysis of new natural coagulant extracts for turbidity removal in water systems. Water Sci Technol. 2025;91(7):797-810. https://doi.org/10.2166/wst.2024.372

Additional information

Peer review: Publisher thanks Sectional Editor and the other anonymous reviewers for their contribution to the peer review of this work.

Reprints & permissions information is available at https://horizonepublishing.com/journals/index.php/PST/open_access_policy

Publisher's Note: Horizon e-Publishing Group remains neutral with regard to jurisdictional claims in published maps and institutional affiliations.

Indexing: Plant Science Today, published by Horizon e-Publishing Group, is covered by Scopus, Web of Science, BIOSIS Previews, Clarivate Analytics, NAAS, UGC Care, etc
See https://horizonepublishing.com/journals/index.php/PST/indexing_abstracting

Publisher information: Plant Science Today is published by HORIZON e-Publishing Group with support from Empirion Publishers Private Limited, Thiruvananthapuram, India.